Plasma Membrane Surface Potential: Dual Effects upon Ion Uptake and Toxicity[1]

Peng Wang, Thomas B. Kinraide, Dongmei Zhou*, Peter M. Kopittke, and Willie J.G.M. Peijnenburg

State Key Laboratory of Soil and Sustainable Agriculture, Institute of Soil Science, Chinese Academy of Sciences, Nanjing 210008, China (P.W., D.Z.); Appalachian Farming Systems Research Center, Agricultural Research Service, United States Department of Agriculture, Beaver, West Virginia 25813–9423 (T.B.K.); University of Queensland, School of Land, Crop, and Food Sciences, St Lucia, Queensland 4072, Australia (P.M.K.); Faculty of Science, Leiden University, 2300 RA Leiden, The Netherlands (W.J.G.M.P.); National Institute of Public Health and the Environment, 3720 Bilthoven, The Netherlands (W.J.G.M.P.); and Graduate School of the Chinese Academy of Sciences, Beijing 100049, China (P.W.)

Electrical properties of plasma membranes (PMs), partially controlled by the ionic composition of the exposure medium, play significant roles in the distribution of ions at the exterior surface of PMs and in the transport of ions across PMs. The effects of coexisting cations (commonly Al^{3+}, Ca^{2+}, Mg^{2+}, H^+, and Na^+) on the uptake and toxicity of these and other ions (such as Cu^{2+}, Zn^{2+}, Ni^{2+}, Cd^{2+}, and $H_2AsO_4^-$) to plants were studied in terms of the electrical properties of PMs. Increased concentrations of cations or decreased pH in rooting media, whether in solution culture or in soils, reduced the negativity of the electrical potential at the PM exterior surface (ψ_0^o). This reduction decreased the activities of metal cations at the PM surface and increased the activities of anions such as $H_2AsO_4^-$. Furthermore, the reduced ψ_0^o negativity increased the surface-to-surface transmembrane potential difference, thus increasing the electrical driving force for cation uptake and decreasing the driving force for anion uptake across PMs. Analysis of measured uptake and toxicity of ions using electrostatic models provides evidence that uptake and toxicity are functions of the dual effects of ψ_0^o (i.e. altered PM surface ion activity and surface-to-surface transmembrane potential difference gradient). This study provides novel insights into the mechanisms of plant-ion interactions and extends current theory to evaluate ion bioavailability and toxicity, indicating its potential utility in risk assessment of metal(loid)s in natural waters and soils.

Some solutes in growth media, such as cations and organic matter, influence the bioavailability and toxicity of metals in natural waters and soils (Peijnenburg et al., 1997; Weng et al., 2004; Kopittke et al., 2010). Novel insights into the bioavailability and toxicity of metals have inspired the development of models in order to allow accurate impact assessments of metals emitted into the environment. The biotic ligand model (BLM; Di Toro et al., 2001), as an extension of the free ion activity model (FIAM), incorporates site-specific competitions among cations (commonly Ca^{2+}, Mg^{2+}, and H^+) and ionic toxicants (commonly heavy metals) for binding to a biotic ligand at the cell surface. The scientific and regulatory communities have become interested in the BLM and have incorporated it into regulations. However, the BLM as the main determinant of toxicant bioavailability does not deserve uncritical acceptance, and the mechanism of the ameliorative effectiveness of cations must be considered carefully, especially in light of cation enhancement of anion toxicity (Kinraide, 2006). Previous studies (Kinraide, 2006; Wang et al., 2008) showed that global electrostatic interactions at the plasma membrane (PM) exterior surfaces, rather than site-specific mechanisms, may play the dominant role in the phytotoxicity of metals.

The process of metal uptake typically encompasses diffusion of the ion to the cell surface, speciation reactions, electrostatic interactions, and subsequent transport across PMs (Hille, 2001; Kinraide, 2001). The PM electrical properties play key roles in the distribution of ions at the exterior surface of PMs, in ion transport across PMs, and, hence, in ion intoxication. Three global electrical features of PMs have been recognized (Fig. 1, top; Kinraide, 2001). The first includes the negative electrical potentials at the PM exterior and interior surfaces (ψ_0^o and ψ_0^i, respectively). The second is the electrical potential difference through the PM from surface to surface ($E_{m,surf}$). The last is the transmembrane electrical potential (E_m) from bulk medium to cell interior. E_m is composed of three potential differences ($E_m = E_{m,surf} + \psi_0^o - \psi_0^i$) and can be measured comparatively easily by the insertion of microelectrodes into cells (Nobel, 1991). The cell wall

[1] This work was supported by the National Natural Science Foundation (grant no. 40871115), the Natural Science Foundation of Jiangsu Province (grant no. BK 2009339), and the Graduate Innovative Program of the Graduate School of the Chinese Academy of Sciences.

* Corresponding author; e-mail dmzhou@issas.ac.cn.

The author responsible for distribution of materials integral to the findings presented in this article in accordance with the policy described in the Instructions for Authors (www.plantphysiol.org) is: Dongmei Zhou (dmzhou@issas.ac.cn).

www.plantphysiol.org/cgi/doi/10.1104/pp.110.165985

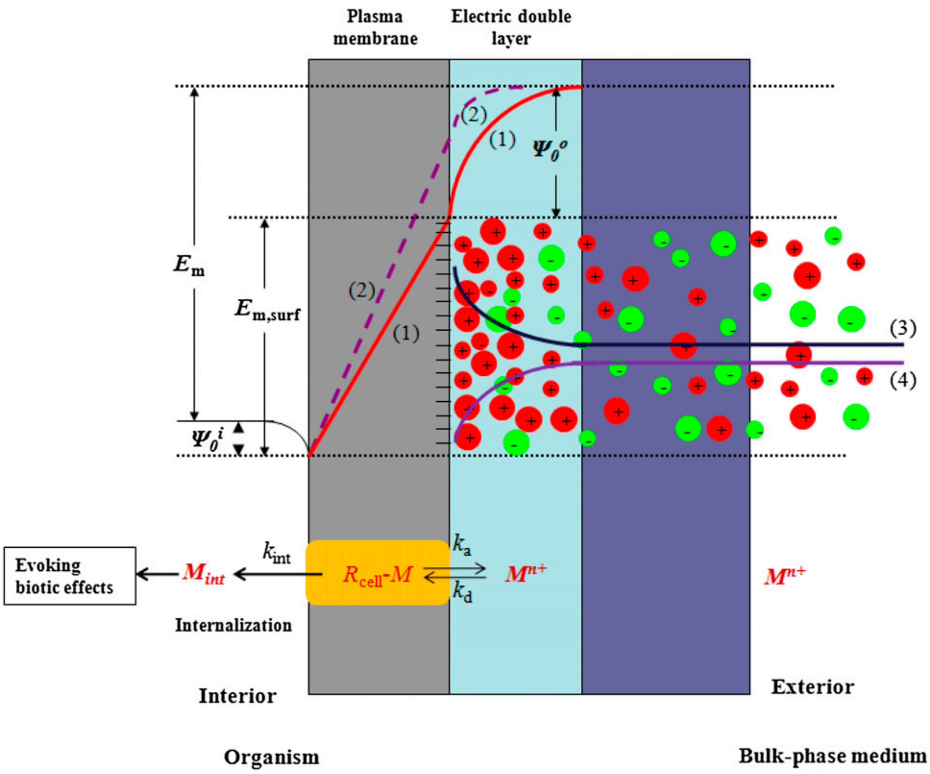

Figure 1. Top, Profile of the electrical potentials and ion distributions at the PM. Bottom, Conceptualized ion (M^{n+}) transport across the PM, including dissociation/association with the active binding site (R_{cell}; e.g. transporter, ion channel) on the surface of the PM. Lines 1 and 2 illustrate the potential profile through the PM and electric double layer before (line 1) and after (line 2) the addition of depolarizing solutes to the bulk-phase medium. $\psi_0{}^o$ is the potential difference between the bulk-phase medium and the external PM surface. E_m is the transmembrane potential difference from the bulk-phase medium to the cell interior. $E_{m,surf}$ is the potential difference through the PM from surface to surface for line 1 ($E_{m,surf}$ is not shown for line 2). The cell wall has been omitted for simplicity. Lines 3 (cations) and 4 (anions) represent the profile of activities from the bulk solutions to the PM exterior surface. k_a, k_d, and k_{int} are the association, dissociation, and internalization rate constants, respectively.

appears to have comparatively little influence on $\psi_0{}^o$ and ion concentrations at the PM surface (Gage et al., 1985; Shomer et al., 2003; Kinraide, 2004). Hence, $\psi_0{}^o$ is controlled by the composition of the soil solution and little, or not at all, by soil solid matter lying external to the cell walls, except as that solid matter influences the soil solution.

Both $\psi_0{}^o$ and $E_{m,surf}$ are physiologically important, because electrical potential gradients influence the distribution and transport and, hence, the biotic effects of ions. The $\psi_0{}^o$ is often sufficiently negative to concentrate cations and deplete anions at the PM surface by more than 10-fold relative to the bulk-phase medium. The ionic composition of the bulk-phase medium influences $\psi_0{}^o$, and cations, commonly Al^{3+}, Ca^{2+}, Mg^{2+}, Na^+, and H^+, reduce the negativity of $\psi_0{}^o$ by charge screening and ion binding. Values for $\psi_0{}^o$ in soil-grown plants range widely because of large variations in soil solution concentrations of cations (Wolt, 1994; Kinraide, 2003b).

$E_{m,surf}$ influences ion channel gating and the driving force for ion fluxes across the PM (Hille, 2001; Kinraide, 2001). A consideration of physiological effects (such as ion uptake and intoxication) upon roots only in terms of activities in the bulk-phase medium can be misleading. The common neglect of $\psi_0{}^o$ is inconsistent with its importance and may reflect the difficulty of measuring $\psi_0{}^o$. Nevertheless, several studies have considered physiological phenomena in terms of $\psi_0{}^o$ (Barber, 1980; McLaughlin, 1989; Zhang et al., 2001; Kinraide, 2003a, 2006; Yermiyahu and Kinraide, 2005; Wang et al., 2008; Kinraide and Wang, 2010; Kopittke et al., 2010), and a fully parameterized Gouy-Chapman-Stern (GCS) model is now available for calculating $\psi_0{}^o$ (Wang et al., 2008; Kinraide and Wang, 2010).

The aims of this study were (1) to emphasize the importance of the PM electrical properties for the transport and toxicity of ions while developing electrostatic models for uptake and toxicity, (2) to determine possible multiple effects of $\psi_0{}^o$ upon ion uptake and toxicity, and (3) to apply electrostatic models, incorporating membrane surface-to-surface activities and electrical gradients, to predict the uptake and toxicity of metal ions for use in risk assessment in natural waters and soils.

THEORY

Calculation of $\psi_0{}^o$ and Ion Activities at the PM Exterior Surface

The GCS model combines electrostatic theory (Gouy-Chapman theory) with ion binding (Stern model) so that $\psi_0{}^o$ can be computed (Tatulian, 1999; Yermiyahu and Kinraide, 2005; Kinraide and Wang, 2010). For a clear introduction to electrostatic theory presented without the restraints upon space required here, we recommend the book chapter by Yermiyahu and Kinraide (2005), and we recommend Barber (1980) and Tatulian (1999) for clear, more in-depth theoretical treatments. This model incorporates the intrinsic surface charge density (σ_0) of a membrane, the ion composition of the bulk-phase medium, and ion binding to the membrane. A detailed analysis (Kinraide and

Wang, 2010) indicates the suitability of $\sigma_0 = -30$ mC m^{-2} while also noting small variability among membranes. A computer program for the GCS model may be obtained from the authors. Knowledge of ψ_0° enables the calculation of ion activities at the PM exterior surface. The activity of ion I^Z at the PM exterior surface ($\{I^Z\}_0^{\circ}$) is computed from the activity of I^Z in the bulk-phase medium ($\{I^Z\}_b$) according to the Nernst equation $\{I^Z\}_0^{\circ} = \{I^Z\}_b \exp[-ZF\psi_0^{\circ}/(RT)]$, where Z is the charge on ion I, F is the Faraday constant, R is the gas constant, and T is temperature. $F/(RT) = 25.7$ when ψ_0° is expressed in mV and $T = 25°C$.

Development of Electrostatic Models of Ion Uptake and Toxicity

Electrostatic Uptake Model

To evoke a biotic effect (e.g. transport, toxicity, alleviation of toxicity, enzyme activity), a metal ion must first react with physiologically active sites, R_{cell} (e.g. transporter, ion channel, enzyme), on the PM surface, often but not necessarily followed by uptake (Fig. 1, bottom).

$$M + R_{cell} \underset{K_d}{\overset{K_a}{\rightleftarrows}} M - R_{cell} \xrightarrow{K_{int}} M_{int} + R_{cell} \longrightarrow \boxed{\text{Evoke biotic effects}} \quad (1)$$

$$J_{uptake} = k_{int}\,[M - R_{cell}] = k_{int}[R_{cell}]_t\,\{M\}_b/(K_m + \{M\}_b),$$
$$\text{where } K_m = (k_d + k_{int})/k_a \quad (2)$$

where J_{uptake} is the ion influx, M_{int} represents the metal taken up with concurrent recycling of R_{cell}, $\{M\}_b$ is the activity of metal in the bulk-phase medium, $[M - R_{cell}]$ is the surface density (mol m^{-2}) of metal bound to R_{cell} (all charges omitted for simplicity), and $[R_{cell}]_t$ is the metal-binding capacity of R_{cell}; k_a, k_d, and k_{int} are the association, dissociation, and uptake rate constants. The conditional stability constant $K_{m\text{-}Rcell}$ for the binding of the metal to R_{cell} at the external PM surface can be denoted as $K_{m\text{-}Rcell}$ ($= k_a/k_d$). In most cases, $k_{int} << k_d$, so that $K_m \approx k_d/k_a = 1/K_{m\text{-}Rcell}$. Equation 2 resembles the Michaelis-Menten equation that is often used to describe steady-state uptake in models such as the FIAM. However, other uptake models, expressing saturation by substrate, have been proposed (Hille, 2001; Kinraide, 2001), and other models may be equally suitable for our analyses (see Eq. 9 below). Specifically, the precise nature of the $M - R_{cell}$ complex is not essential. $M - R_{cell}$ may also be envisioned as restricted flow through a channel rather than an actual metal-ligand binding. The important feature of our analysis is the impact of ψ_0° upon k_{int}, as developed next.

Commonly, metal ion transport across PMs is expressed in terms of k_{int} and its activity in the bulk-phase medium ($\{M\}_b$), rather than the activity at the PM exterior surface ($\{M\}_0^{\circ}$), but root responses to ions often correlate poorly with $\{M\}_b$ and often correlate well with $\{M\}_0^{\circ}$ (Zhang et al., 2001; Yermiyahu and Kinraide, 2005; Wang et al., 2008; Kinraide and Wang, 2010; Kopittke et al., 2010). Furthermore, the k_{int} is influenced by the electrical driving force on the ion (i.e. $E_{m,surf}$). Therefore, the objective of this study was to ascertain the dual effects of changes in ψ_0° (changes in PM surface activity of ions and changes in $E_{m,surf}$), independent of changes in E_m, upon ion uptake and intoxication. To do so, Equation 2 was modified.

Initially, Equation 2 was modified to take into account the effect of ψ_0° on the enrichment of cations and depletion of anions at the PM surface. This was accomplished by replacing $\{M\}_b$ with $\{M\}_0^{\circ}$.

$$J_{uptake} = k_{int}\,[R_{cell}]_t\,\{M\}_0^{\circ}/(K_m + \{M\}_0^{\circ}) \quad (3)$$

The internalization constant k_{int} resembles in some ways $P_jZFE_{m,surf}/(RT)$ in a modified Goldman-Hodgkin-Katz flux equation (Kinraide, 2001), where P_j is a permeability coefficient. Thus, k_{int} is proportional to $E_{m,surf}$, which may be computed from $E_{m,surf} = E_m - \psi_0^{\circ} + \psi_0^{i}$. E_m remained essentially constant under the conditions of our experiments, or changes were small or transient (Llamas et al., 2000; Kinraide, 2001). ψ_0^{i} was small (≈ -10 mV), and changes were small relative to changes in ψ_0° because of high [Mg^{2+}], high ionic strength, and constant pH in the cytoplasm (Marschner, 1995). Therefore, $E_{m,surf} = A - \psi_0^{\circ}$, where A is a constant equal to $E_m + \psi_0^{i}$. Uptake, therefore, was driven by both the PM surface activity of ions and ψ_0°, the latter as a surrogate for $E_{m,surf}$. Accordingly, Equation 3 was modified, yielding the electrostatic uptake model (EUM):

$$\begin{aligned} J_{uptake} &= k_{int}\,[R_{cell}]_t\{M\}_0^{\circ}/(K_m + \{M\}_0^{\circ}) \\ &= kE_{m,surf}\,[R_{cell}]_t\{M\}_0^{\circ}/(K_m + \{M\}_0^{\circ}) \\ &= a\,(1 + b\psi_0^{\circ})\{M\}_0^{\circ}/(K_m + \{M\}_0^{\circ}) \end{aligned} \quad (4)$$

where $a = k[R_{cell}]_tA$ and $b = -1/A$.

Electrostatic Toxicity Model

When growth responds to measures of toxicant intensity, the resulting curves are often downwardly sigmoidal and can be expressed in the following equation where growth is limited by $\{M\}_b$ and is expressed as relative root elongation (RRE; as percentage of nonintoxicated growth):

$$\text{RRE} = 100/\exp[(\alpha\{M\}_b)^{\beta}] \quad (5)$$

where α is a strength coefficient that increases with the strength of the metal toxicity and β is a shape coefficient that confers sigmoidality when its value is greater than 1. Using $\{M\}_0^{\circ}$ rather than $\{M\}_b$ takes into account the effect of ψ_0° on the enrichment of cations and depletion of anions. Thus, Equation 5 becomes

$$\text{RRE} = 100/\exp[(\alpha\{M\}_0^{\circ})^{\beta}] \quad (6)$$

This versatile equation adequately represents dose responses to most toxicants (see figure 8 in Yermiyahu and Kinraide, 2005). The electrical component of the driving force may be incorporated into Equation 6 by expanding the coefficient α to include $\psi_0^{\ o}$, yielding the electrostatic toxicity model (ETM):

$$\mathrm{RRE} = 100/\exp\{[\alpha(1 + b\psi_0^{\ o})\{M\}_0^{\ o}]^{\beta}\} \quad (7)$$

Equations 4 and 7 now incorporate the dual effects of $\psi_0^{\ o}$ on ion uptake and toxicity, namely, the effects upon the enrichment of cations or depletion of anions at the PM surface and upon the driving force across the PM. It is noteworthy that sometimes large differences in uptake and tolerance are observed among plant species. The differences in the α and β coefficients for Equations 4 and 7 may denote differences in uptake and sensitivity. In the case of cationic uptake and toxicity, we would expect coefficient b to have a positive value so that increasing values of $\psi_0^{\ o}$ (i.e. decreasing negativity of $\psi_0^{\ o}$, resulting in increasing negativity of $E_{m,surf}$) will increase k_{int}, causing J_{uptake} to increase and RRE to decrease. In the case of anions, we would expect a negative value for b. All coefficients in Equations 2 through 7 were evaluated by regression analysis so that r^2 and the statistical significance of the coefficients could be evaluated. No coefficients are reported whose 95% confidence intervals encompassed 0.

RESULTS AND DISCUSSION

Effects of Coexistent Cations on Electrical Potentials and the Uptake and Toxicity of Copper

As expected, increases in Ca^{2+}, Mg^{2+}, or H^+ reduced Cu^{2+} uptake and toxicity (experiments 3 and 11, Table I). Increases in Ca^{2+} concentrations from 0.25 to 4.0 mM significantly decreased the 48-h uptake of Cu^{2+} by wheat (*Triticum aestivum* 'Yangmai 14') roots (Fig. 2A). In addition, the 48-h EA50$\{Cu^{2+}\}_b$ (i.e. the activity of Cu^{2+} in the bulk-phase medium causing a 50% reduction in growth in 48 h) increased from 0.68 to 1.6 μM (Fig. 2B). Similar results were observed with increasing $\{Mg^{2+}\}_b$ and decreasing pH (data not shown). To elucidate $\psi_0^{\ o}$ effects, we computed the 48-h EA50$\{Cu^{2+}\}_0^{\ o}$ (i.e. the activity of Cu^{2+} at the external surface of the PM causing a 50% reduction). These values for 48-h EA50$\{Cu^{2+}\}_0^{\ o}$ reflect the intrinsic sensitivity of roots to metals, but note that a decrease in EA50$\{Cu^{2+}\}_0^{\ o}$ reflects an increase in sensitivity. Interestingly, the intrinsic sensitivity of Cu^{2+} was increased significantly with increasing Ca^{2+}, with the 48-h EA50$\{Cu^{2+}\}_0^{\ o}$ decreasing from 21.1 to 7.4 μM (Fig. 2C). This was consistent with our previous studies that also demonstrated that the extrinsic sensitivity to Cu^{2+} (sensitivity to $\{Cu^{2+}\}_b$) decreased as $\psi_0^{\ o}$ became less negative and that the intrinsic sensitivity to Cu^{2+} (sensitivity to $\{Cu^{2+}\}_0^{\ o}$) increased (see figure 7A in Wang et al., 2008), but those effects were not explained. Reanalysis of previous studies demonstrates that decreased $\psi_0^{\ o}$ negativity enhances the intrinsic toxicity of Cu^{2+} (Lock et al., 2007a), Co^{2+} (Lock et al., 2007b), and Ni^{2+} (Lock et al., 2007c) to barley (*Hordeum vulgare*).

We propose that this increase in intrinsic sensitivity caused by reductions in $\psi_0^{\ o}$ negativity results from increases in the $E_{m,surf}$ negativity; this would increase the electrical driving force for cationic influxes (Fig. 3). Changes in $\psi_0^{\ o}$ have little impact on E_m (Llamas et al., 2000; Hille, 2001; Kinraide, 2001), in contrast to effects upon $E_{m,surf}$. Consequently, changes in $\psi_0^{\ o}$ are offset almost entirely by changes in $E_{m,surf}$ (compare solid and dashed lines in Fig. 3, where $E_{m,surf} = E_m - \psi_0^{\ o} + \psi_0^{\ i}$). Thus, the decreased negativity of $\psi_0^{\ o}$ resulted in reduced attraction of Cu^{2+} to the PM surface (the $\{Cu^{2+}\}_0^{\ o}$ decreased from 38.3 to 1.1 μM; Fig. 3B), and hence a decreased extrinsic sensitivity, but the decreased negativity of $\psi_0^{\ o}$ caused an increase in the negativity of $E_{m,surf}$, and hence an increased intrinsic sensitivity.

Modeling Ion Uptake and Toxicity with Electrostatic Models (EUM and ETM)

Cu^{2+} Uptake and Toxicity Affected by Ca^{2+}, Mg^{2+}, or pH

Figure 4 illustrates Cu^{2+} uptake and toxicity as functions of $\{Cu^{2+}\}_b$ (Fig. 4, A and E), $\{Cu^{2+}\}_0^{\ o}$ (Fig. 4, B and F), and calculated Cu^{2+} uptake and toxicity based on the EUM (Eq. 4) and ETM (Eq. 7; Fig. 4, C and G). The Cu^{2+} uptake corresponds to the calculated Cu^{2+} uptake (r^2 = 0.949; Fig. 4C) more closely than to $\{Cu^{2+}\}_0^{\ o}$ (r^2 = 0.867; Fig. 4B) or $\{Cu^{2+}\}_b$ (r^2 = 0.840; Fig. 4A). For toxicity, RRE correlates better with calculated RRE (r^2 = 0.956; Fig. 4G) than with $\{Cu^{2+}\}_0^{\ o}$ (r^2 = 0.794; Fig. 4E) or $\{Cu^{2+}\}_b$ (r^2 = 0.843; Fig. 4F). Also, Figure 4 illustrates the uptake (Fig. 4D) and the RRE (Fig. 4H) as functions of $\psi_0^{\ o}$ and $\{Cu^{2+}\}_0^{\ o}$. The curved surfaces are based on the electrostatic uptake and toxicity models using the parameters in Tables II and III (experiments 3 and 11).

Ca^{2+} Uptake Affected by Al^{3+}, La^{3+}, Mg^{2+}, or Sr^{2+}

Huang et al. (1994, 1996) measured radiotracer Ca^{2+} influx into right-side-out PM vesicles from wheat roots (cv Scout 66) in response to variable external Ca^{2+}, Al^{3+}, La^{3+}, Mg^{2+}, Sr^{2+}, and pH. E_m was controlled by the adjustment of internal and external K^+, which, with valinomycin, clamped E_m at –100 mV. Their data demonstrate the well-known inhibitory effect of Al^{3+}, La^{3+}, Mg^{2+}, and Sr^{2+} on short-term (5-min) Ca^{2+} uptake, which is commonly attributed to blockade or competition at a Ca^{2+} channel. However, we question whether the inhibition occurs as a consequence of channel blockade (or competition) or as a consequence of electrostatic reduction of $\{Ca^{2+}\}_0^{\ o}$. An analysis of published patch-clamp studies (Kinraide, 2001) revealed that inhibition of Ca^{2+} uptake usually entails reduced unitary channel conductance rather than a reduced probability of channel openness (i.e. true blockade).

In order to investigate the possible dual effects of $\psi_0^{\ o}$, measured Ca^{2+} uptake was plotted against $\{Ca^{2+}\}_b$

Table I. *Overview of studies used to examine ion uptake and toxicity*

For each study, the pH, total concentration of ions ($[I]_t$), and the calculated ψ_0^o are reported. The ψ_0^o was calculated for each medium with the standard GCS model.

Species and Source	Experiment No.	pH	$[Al]_t$ or $[La]_t$	$[CaCl_2]_t$	$[Mg]_t$ or $[Sr]_t$	$[NaCl]_t$	ψ_0^o
			μM	mM	mM	mM	mV
Ca^{2+} influx into PM vesicles of wheat roots (Huang et al., 1994)	1	7.0	$[AlCl_3]$ 0–20	0.01–5.0	$[MgCl_2]$ 0–0.5 $[SrCl_2]$ 0–0.5		–87.6 to –18.9
Ca^{2+} influx into PM vesicles of wheat roots (Huang et al., 1996)	2	4.5	$[LaCl_3]$ 0–20	0.01–3.0			–34.7 to –5.49
Cu^{2+} uptake by wheat seedlings (this study)	3	5.1–6.0		0.25–3.8	$[MgCl_2]$ 0.26–4.0	1.0	–44.4 to –19.3
Zn^{2+} uptake by pea seedlings (Wu, 2007)	4	4.3–6.0		0.19–1.8			–57.1 to –14.9
Ca^{2+} uptake by wheat roots (Davenport et al., 1997)	5	6.5		0–3.1		5.0–150	–86.4 to –6.6
Na^+ uptake by wheat roots (Davenport et al., 1997)	6	6.5		0.08–11		5.0–150	–61.4 to –6.6
Cd^{2+} uptake by pea seedlings (Wu, 2007)	7	4.0–6.0		0.04–1.6			–76.0 to –8.7
Ni^{2+} uptake by pea seedlings (Wu, 2007)	8	4.0–6.0		0.04–1.8			–76.0 to –8.2
Cu^{2+} uptake by pea seedlings (Wu, 2007)	9	4.0–6.0		0.04–1.9			–75.9 to –8.3
$H_2AsO_4^-$ uptake by wheat seedlings (this study)	10	4.4–6.0		0.24–4.1	$[MgCl_2]$ 0.26–3.7	0.91	–43.8 to –19.1
Cu^{2+} rhizotoxicity to wheat seedlings (this study)	11	5.1–6.0		0.25–3.8	$[MgCl_2]$ 0.26–4.0	1.0	–44.4 to –19.3
Cu^{2+} rhizotoxicity to wheat seedlings (Parker et al., 1998)	12	4.5–6.0		0.20–4.0	$[MgCl_2]$ 0–4.7		–56.6 to –12.7
Cu^{2+} rhizotoxicity to wheat seedlings (Kinraide, 2006)	13	4.5–5.7		0.50–8.0		0 - 10	–33.4 to –8.7
Al^{3+} rhizotoxicity to wheat seedlings (Tyler wheat, archived data)	14	4.3	$[AlCl_3]$ 0–20	0.40–4.0	$[MgCl_2]$ 0–3.6		–25.3 to 0.8
$H_2AsO_4^-$ rhizotoxicity by wheat seedlings (this study)	15	4.5–6.0		0.27–4.3	$[MgCl_2]$ 0.26–4.0	0.53–20	–44.1 to –19.1

and $\{Ca^{2+}\}_0^o$ and against calculated Ca^{2+} uptake based on the EUM (Eq. 4). Figure 5 indicates that Ca^{2+} uptake corresponds to this calculated Ca^{2+} uptake (r^2 = 0.938) more closely than to $\{Ca^{2+}\}_0^o$ (r^2 = 0.775) or to $\{Ca^{2+}\}_b$ (r^2 = 0.458; Table II). Figure 5D illustrates that the Ca^{2+} uptake depended on ψ_0^o and $\{Ca^{2+}\}_0^o$, indicating that the effects of Al^{3+}, La^{3+}, Mg^{2+}, and Sr^{2+} on Ca^{2+} uptake may be attributable to the dual effects of ψ_0^o rather than to a channel blockade or competition. The curved surface (Fig. 5D) is based on the EUM with the parameter values in Table II (experiments 1 and 2).

Na^+ Uptake Affected by Ca^{2+} and Ca^{2+} Uptake Affected by Na^+

Davenport et al. (1997) measured short-term (20-min) and long-term (7-d) Na^+ unidirectional uptake into roots of two species of wheat (*T. aestivum* 'Kharchia' and *Triticum turgidum* 'Modoc') cultured in variable concentrations of NaCl and $\{Ca^{2+}\}_b$. It is clear from their Figures 3, 4, and 5 that Ca^{2+} effectively inhibited Na^+ uptake and vice versa. It was assumed that Na^+ uptake occurred passively via Ca^{2+} channels and that the decreased Na^+ uptake was attributable to Ca^{2+} binding to a specific site on such channels, thereby altering the gating and selectivity of the channels. However, correlation between measured and calculated uptake for both Na^+ and Ca^{2+} was superior when using the EUM (Eq. 4; Table II, experiments 5 and 6). These results indicate that cation effects may be attributed to the dual effects of ψ_0^o rather than to specific blocking effects.

Zn^{2+}, Cu^{2+}, Cd^{2+}, and Ni^{2+} Uptake Affected by Ca^{2+} or pH

In a study with pea (*Pisum sativum* 'Lincoln'), Wu (2007) measured changes in the uptake of Zn^{2+}, Cu^{2+}, Ni^{2+}, and Cd^{2+} in response to added Ca^{2+} and H^+. In nearly all cases, increases in Ca^{2+} or decreases in pH reduced metal uptake. That study measured some characteristics of pea roots and considered theoretical aspects of the FIAM and the BLM. For our reanalysis, uptake data were taken from the author's tables. For the Zn^{2+} uptake experiments, increases in Ca^{2+} concentration or decreases in pH resulted in decreases in

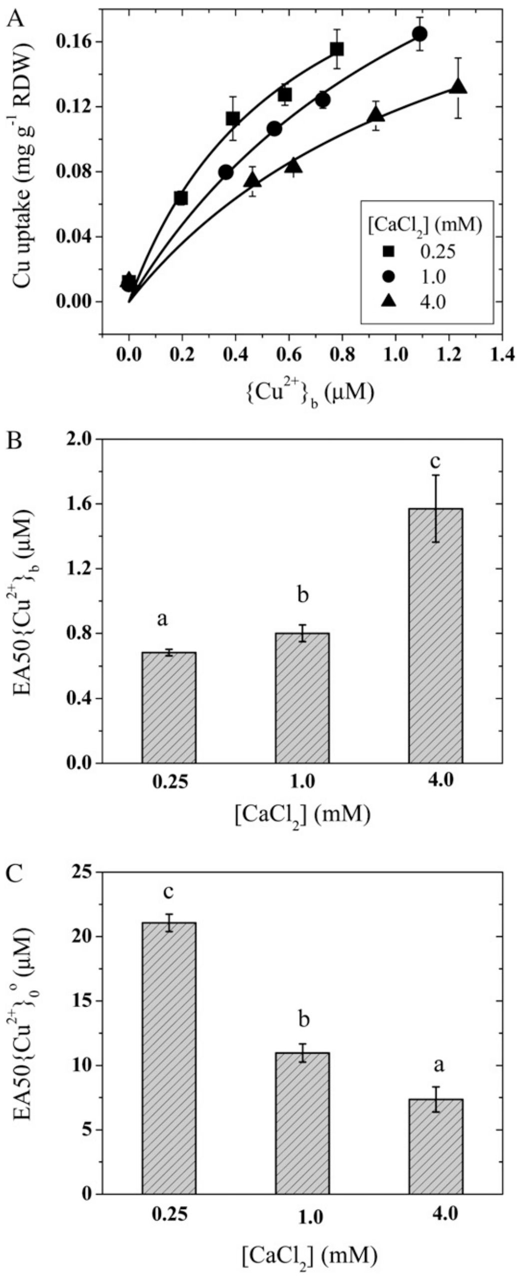

Figure 2. Uptake and toxicity in response to Cu^{2+} and Ca^{2+} in wheat seedlings, showing the uptake of Cu^{2+} as a function of $\{Cu^{2+}\}_b$ at different $[CaCl_2]$ (A), the effect of Ca^{2+} on EA50$\{Cu^{2+}\}_b$ (B), and the effect of Ca^{2+} on EA50$\{Cu^{2+}\}_0$ (C). Error bars indicate 95% confidence intervals. Different letters indicate significant differences among means ($P < 0.01$). Data are from experiments 3 and 11. RDW, Root dry weight.

the negativity of $\psi_0{}^o$ and reductions in Zn^{2+} uptake (data not shown). The measured Zn^{2+} uptake was better correlated with the Zn^{2+} uptake calculated by the EUM ($r^2 = 0.967$) than with $\{Zn^{2+}\}_0{}^o$ ($r^2 = 0.851$) or $\{Zn^{2+}\}_b$ ($r^2 = 0.821$; Table II, experiment 4). Similar results were observed for Cu^{2+}, Ni^{2+}, or Cd^{2+} uptake (Table II, experiments 7–9).

Cu^{2+} Toxicity Affected by Ca^{2+}, Mg^{2+}, Na^+, or pH

Parker et al. (1998) investigated Cu^{2+} rhizotoxicity to roots of wheat (cv Yecora Rojo) in response to variable concentrations of $CuCl_2$, $CaCl_2$, $MgCl_2$, and pH in a factorial array. Increases in Ca^{2+}, Mg^{2+}, or H^+ alleviated Cu^{2+} stress. For our reanalysis, data were taken from their Figures 2 to 5 and Tables I and II. For each data point in the figures and tables, Cu^{2+} and Ca^{2+} concentrations, pH, and relative net elongation were recorded, and $\psi_0{}^o$ and $\{Cu^{2+}\}_0{}^o$ were calculated. Measured RRE correlated more strongly with the calculated RRE based on the ETM (Eq. 7; $r^2 = 0.921$) than with $\{Cu^{2+}\}_0{}^o$ ($r^2 = 0.878$) or $\{Cu^{2+}\}_b$ ($r^2 = 0.745$; Table III, experiment 12). This indicates a dual effect of $\psi_0{}^o$.

Kinraide (2006) presented results from experiments assessing wheat (cv Atlas 66) seedling root elongation in solutions containing variable concentrations of $CuSO_4$, $CaCl_2$, NaCl, and pH. Increases in Ca^{2+}, Na^+, or H^+ in the rooting medium alleviated the Cu^{2+} rhizotoxicity. This study considered the first effect of $\psi_0{}^o$ upon $\{Cu^{2+}\}_0{}^o$ and the possibility of competition at a binding site at the PM surface (BLM). In our reanalysis, RRE correlated more strongly with the calculated RRE based on the ETM (Table III, experi-

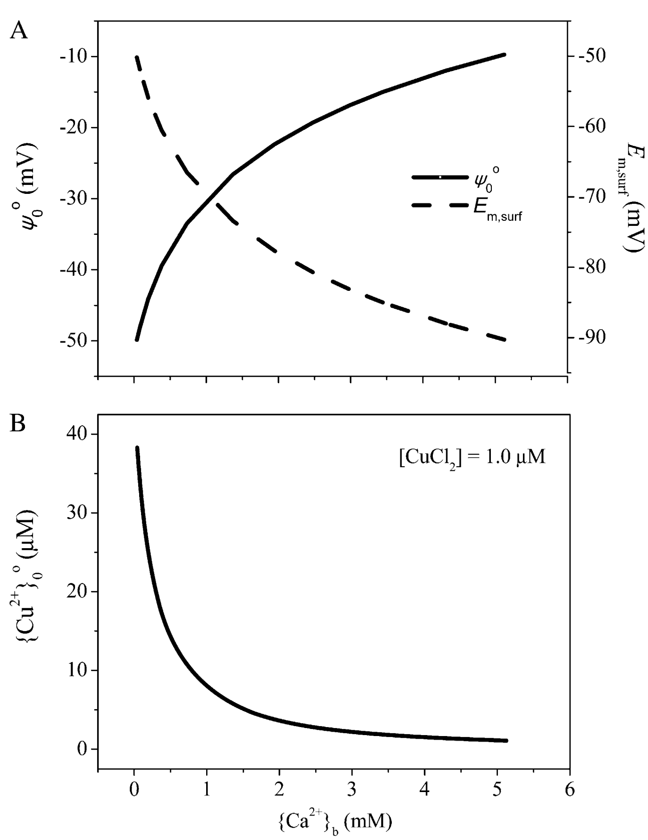

Figure 3. Predicted electrical potential and PM surface activity of Cu^{2+} in response to Ca^{2+} activity in the bulk-phase medium. A, The $\psi_0{}^o$ and $E_{m,surf}$. B, The calculated PM surface activity of Cu^{2+} at 1.0 μM $CuCl_2$. Data are from experiments 3 and 11.

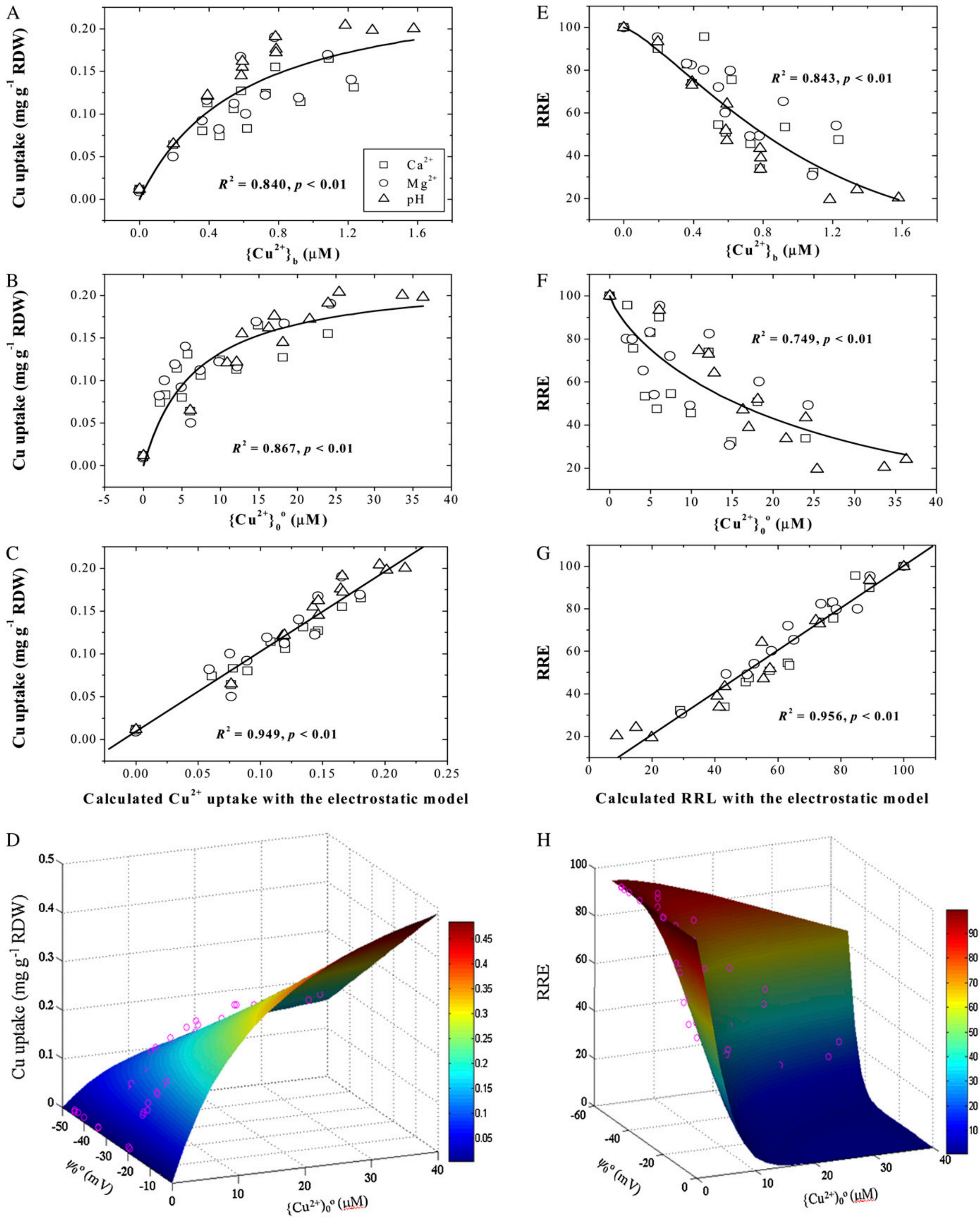

Figure 4. Uptake (left column) and RRE (right column) of Cu^{2+} by wheat roots as functions of $\{Cu^{2+}\}_b$ (first row), $\{Cu^{2+}\}_0^o$ (second row), and Cu^{2+} uptake or RRE calculated from electrostatic models (third row). Uptake and RRE as functions of ψ_0^o and Cu^{2+} surface activity are shown in the bottom row. In D and H, the curved surfaces denote uptake or RRE calculated from the electrostatic models, while the pink circles represent the measured values. Data are from experiments 3 and 11. RDW, Root dry weight.

Table II. *Comparison of three models for ion uptake*

For the FIAM, uptake is expressed in terms of the activity in the bulk-phase rooting medium according to the equation $J_{int} = a\,\{M\}_b/(K_m + \{M\}_b)$. For the SIAM, uptake is expressed in terms of the activity at the PM exterior surface according to the equation $J_{int} = a\,\{M\}_0^o/(K_m + \{M\}_0^o)$. For the EUM, uptake is expressed in terms of the PM surface activity and electrical potentials (ψ_0^o) according to the equation $J_{int} = a\,(1 + b\,\psi_0^o)\,\{M\}_0^o/(K_m + \{M\}_0^o)$. $\{M\}$ refers to one of the ions below; a, K_m, and b are coefficients (a resembles in some ways the J_{max} in the Michaelis-Menten equation); and n is the number of data points. All of the presented values for coefficients are statistically significant (95% confidence intervals do not encompass 0). All units of $\{M\}$ and J_{int} were those used in the references. For experiments 1 and 2, J_{int} was expressed in nmol mg^{-1} min^{-1}; for experiments 3, 4, and 7 to 9, J_{int} was expressed in mg g^{-1} root dry weight; for experiments 5 and 6, J_{int} was expressed in μmol g^{-1} root fresh weight h^{-1}. All activities are expressed in μM except for experiment 6, in which Na^+ activities are expressed in mM.

Ion	Experiment No.	A	K_m	b	n	r^2
FIAM						
Ca^{2+}	1 and 2	9.72	$10^{2.40}$		78	0.458
Cu^{2+}	3	0.258	$10^{-0.22}$		45	0.840
Zn^{2+}	4	0.023			54	0.821
Ca^{2+}	5	0.011			20	0.493
Na^+	6	0.113			32	0.825
Cu^{2+}	7	0.192			54	0.685
Cd^{2+}	8	0.154			45	0.660
Ni^{2+}	9	0.088			54	0.626
SIAM						
Ca^{2+}	1 and 2	8.54	$10^{3.74}$		78	0.775
Cu^{2+}	3	0.223	$10^{0.84}$		45	0.867
Zn^{2+}	4	6.28	$10^{3.35}$		54	0.851
Ca^{2+}	5	0.0027			20	0.767
Na^+	6	0.0580			32	0.846
Cu^{2+}	7	0.0059			54	0.830
Cd^{2+}	8	0.0047			45	0.830
Ni^{2+}	9	0.0019			54	0.834
EUM						
Ca^{2+}	1 and 2	70.9	$10^{4.54}$	0.0112	78	0.938
Cu^{2+}	3	0.676	$10^{1.19}$	0.0136	45	0.949
Zn^{2+}	4	56.7	$10^{4.06}$	0.0157	54	0.967
Ca^{2+}	5	0.0043		0.0135	20	0.908
Na^+	6	0.0776		0.0125	32	0.901
Cu^{2+}	7	0.0186		0.0130	54	0.938
Cd^{2+}	8	0.0104		0.0104	45	0.890
Ni^{2+}	9	0.0076		0.0120	54	0.906

ment 13) than with $\{Cu^{2+}\}_0^o$ or $\{Cu^{2+}\}_b$, suggesting that the ameliorative effectiveness of Ca^{2+}, Na^+, and H^+ results from the dual effects of ψ_0^o.

Al^{3+} Toxicity Affected by Ca^{2+}, Mg^{2+}, or pH

We reevaluated the Ca^{2+} and Mg^{2+} alleviation of Al^{3+} rhizotoxicity in wheat (cv Tyler) roots from data archived from, but not presented in, a study by Kinraide and Parker (1987). Two-day-old seedlings were transferred to solutions containing 0.4 mM $CaCl_2$ at pH 4.3 variously supplemented with $AlCl_3$ and $MgCl_2$ or additional $CaCl_2$. Addition of Ca^{2+} or Mg^{2+} alleviated Al^{3+} toxicity. Kinraide et al. (1992) reassessed the interactive effects of Ca^{2+} and Mg^{2+} on Al^{3+} toxicity in terms of ψ_0^o and demonstrated that the ψ_0^o plays an important role in Al^{3+}-Ca^{2+} and Al^{3+}-Mg^{2+} interactions by the first effect of ψ_0^o: the enhancement of cations at the PM surface. For our reanalysis, the dual effects were considered simultaneously in the ETM. Again, the correlation between measured and calculated Al^{3+} toxicity was significantly improved (Fig. 6; Table III, experiment 14), indicating that the Ca^{2+} and Mg^{2+} alleviation of Al^{3+} toxicity may be attributed to effects upon both $E_{m,surf}$ and $\{Al^{3+}\}_0^o$ (i.e. the dual effects of ψ_0^o).

Anion $H_2AsO_4^-$ Uptake and Toxicity Affected by Ca^{2+}, Mg^{2+}, Na^+, or pH

The addition of Ca^{2+} or Mg^{2+} or the reduction of pH will increase the surface activity of $H_2AsO_4^-$ and thus the uptake and toxicity of arsenic. $H_2AsO_4^-$ (arsenate) may become transformed in the roots into the even more toxic $H_2AsO_3^-$ (arsenite; Pickering et al., 2000). Further transformation, translocation, and secretion from the roots may provide some relief of arsenic toxicity. Even so, one would expect ψ_0^o to have an effect upon arsenic uptake, retention, and toxicity. Our hypothesis was that the effects of ψ_0^o upon anionic arsenic toxicants would be opposite to the effects upon cationic toxicants.

Table III. *Comparison of three models for ion toxicity*

For the FIAM, toxicity is expressed in terms of the activity in the bulk-phase rooting medium according to the equation RRE = $100/\exp[(\alpha\{M\}_b)^{\beta}]$. For the SIAM, toxicity is expressed in terms of the activity at the PM exterior surface according to the equation RRE = $100/\exp[(\alpha\{M\}_0{}^{o})^{\beta}]$. For the ETM, toxicity is expressed in terms of the PM surface activity and electrical potentials ($\psi_0{}^{o}$) according to the equation RRE = $100/\exp\{[\alpha(1 + b\psi_0{}^{o})\{M\}_0{}^{o}]^{\beta}\}$. $\{M\}$ refers to one of the ions below; α, β, and b are coefficients: α is a strength coefficient and β is a shape coefficient. All of the presented values for coefficients are statistically significant (95% confidence intervals do not encompass 0). All activities are expressed in μM.

Ion	Experiment No.	α	β	b	n	r^2
FIAM						
Cu^{2+}	11	0.933	1.29		45	0.843
Cu^{2+}	12	1.69	0.901		51	0.745
Cu^{2+}	13	1.72	2.32		36	0.654
Al^{3+}	14	0.227	1.21		50	0.660
$H_2AsO_4^-$	15	0.456	1.95		100	0.903
SIAM						
Cu^{2+}	11	0.040	0.781		45	0.749
Cu^{2+}	12	0.122	0.639		51	0.878
Cu^{2+}	13	0.312	1.88		36	0.835
Al^{3+}	14	0.143	3.26		50	0.919
$H_2AsO_4^-$	15	1.82	1.57		100	0.919
ETM						
Cu^{2+}	11	0.210	1.43	0.0187	45	0.956
Cu^{2+}	12	0.281	0.908	0.0143	51	0.921
Cu^{2+}	13	0.552	2.36	0.0186	36	0.889
Al^{3+}	14	0.155	3.63	0.0164	50	0.949
$H_2AsO_4^-$	15	0.628	1.94	−0.0607	100	0.937

Indeed, an increase in Ca^{2+} from 0.25 to 4.0 mM decreased the 48-h EA50$\{As(V)\}_b$ from 2.9 to 1.7 μM, indicating an increased extrinsic sensitivity. In contrast, the corresponding EA50$\{As(V)\}_0{}^{o}$ increased from 0.48 to 1.49 μM, indicating a decreased intrinsic sensitivity. In contrast to Cu^{2+}, As(V) uptake was sigmoidal and thus did not comply with the Michaelis-Menten equation. This may be related to the concentrations used in our treatments and to hormesis by As(V) (Calabrese, 2008; Wang et al., 2008), which was always observed in low-arsenic treatments. A stimulation of root elongation would dilute the As(V) concentration in roots. Therefore, the uptake of As(V) was expressed using a generalized sigmoidal equation:

$$J_{\mathrm{uptake}} = J_{\max}\,\{1 - 1/\exp[(\alpha\{\mathrm{H_2AsO_4^-}\}_{\mathrm{b}})^{\beta}]\} \quad (8)$$

where J_{max} is the maximum influx, which occurs when $\{As(V)\}_b$ is very large, and α and β resemble their counterparts in Equation 5. Regression analysis with Equation 8 for As(V) uptake yielded r^2 = 0.830. Subsequently, $\{H_2AsO_4^-\}_b$ was replaced with $\{H_2AsO_4^-\}_0{}^{o}$ to include the first effect of $\psi_0{}^{o}$ upon the depletion of anions at the PM surface, and the coefficient α was expanded to $\alpha(1 + b\psi_0{}^{o})$ to incorporate the electrical component of the driving force (the second effect of $\psi_0{}^{o}$).

$$J_{\mathrm{uptake}} = J_{\max}\,\{1 - 1/\exp[(\alpha(1 + b\psi_0{}^{o})\{\mathrm{H_2AsO_4^-}\}_0{}^{o})^{\beta}]\} \quad (9)$$

In the case of anionic toxicants, b is expected to be negative, so that a decreasing negativity of $\psi_0{}^{o}$ will decrease the value of the expanded coefficient, causing J_{uptake} to decrease. Regression analysis with Equation 9 indeed produced a negative value for b (–0.0649) and an increase in r^2 to 0.910 (Table II, experiment 10).

To assess As(V) toxicity, the measured RRE was plotted against RRE calculated on the basis of the ETM (Eq. 7) to estimate the dual effects of $\psi_0{}^{o}$. The correlation between RRE and the model-calculated RRE (r^2 = 0.937) was superior to the correlation between RRE and $\{H_2AsO_4^-\}_0{}^{o}$ (r^2 = 0.919) or $\{H_2AsO_4^-\}_b$ (r^2 = 0.903; Table III, experiment 15). As expected, the regression analysis also yielded a negative value for b in Equation 7 (b = –0.0607, close to the value of –0.0649 reported for the EUM [i.e. b in Eq. 9]).

A Dual Role for $\psi_0{}^{o}$ Expressed in Soil Culture

A dual role for $\psi_0{}^{o}$ appears to be expressed in soil cultures as well as in solution cultures. Ninety-four soil samples were collected from various horizons and soil series from forests in Appalachia, in the northeastern United States, The Netherlands, Sweden, and Germany (Kinraide, 2003b). Some of the soils were used in growth experiments, and growth of wheat (cv Hart), switchgrass (*Panicum virgatum* 'Cave-Rock'), and subterranean clove (*Trifolium subterraneum* 'Mt. Barker') was assessed in terms of the extracted soil solutions. The plant growth in these soils was dependent on the Al^{3+} toxicity and H^+ toxicity and on Ca^{2+} deficiency. A reanalysis of those data demonstrates the dual influence of $\psi_0{}^{o}$ upon plant growth. When the α coefficient was expanded to $\alpha_1(1 + b\psi_0{}^{o})$ in the growth

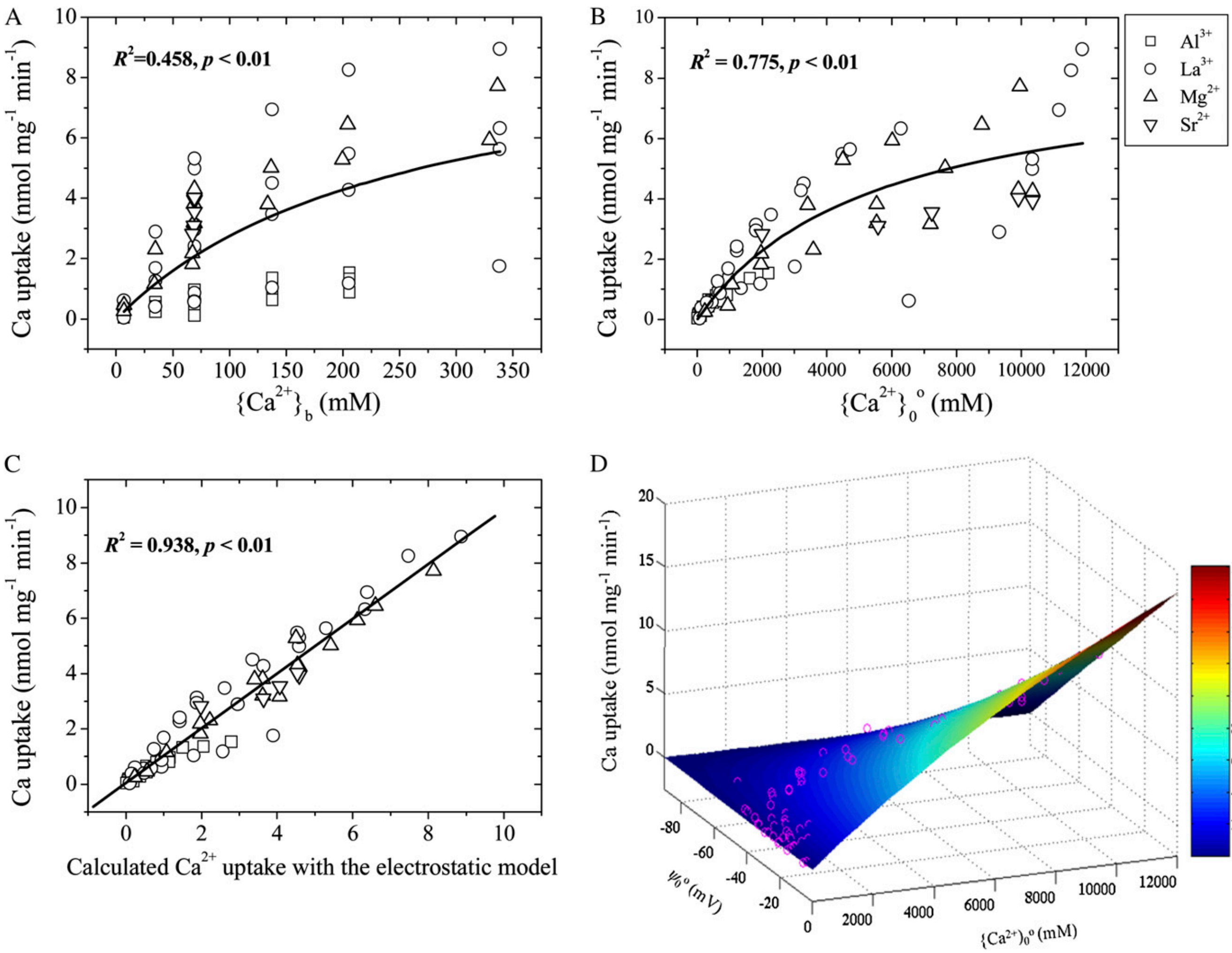

Figure 5. Measured Ca^{2+} uptake plotted against $\{Ca^{2+}\}_b$ (A), $\{Ca^{2+}\}_0{}^o$ (B), or Ca^{2+} uptake calculated from the EUM (Eq. 4; C) or as a function of $\psi_0{}^o$ and $\{Ca^{2+}\}_0{}^o$ (D). In D, the curved surface denotes uptake calculated with the EUM, while the pink circles represent the measured uptake. Data are from Huang et al. (1994, 1996; experiments 1 and 2), who measured Ca^{2+} influx into PM vesicles from wheat roots in a basal medium of 0.1 mM NaCl and 1.0 mM K_2SO_4 at pH 7.0 (for La^{3+}, Mg^{2+}, and Sr^{2+}) or pH 4.5 (for Al^{3+}). The E_m in all solutions was clamped at a constant –100 mV.

equations ($RRE_{Al} = 100/\exp[(\alpha\{Al^{3+}\}_0{}^o)^\beta]$, $RRE_H = 100/\exp[(\alpha\{H^+\}_0{}^o)^\beta]$, and $RRE_{Ca} = 100\{1 - 1/\exp[(\alpha\{Ca^{2+}\}_0{}^o)^\beta]\}$), the r^2 increased by 0.315 (from 0.340 to 0.655), 0.294 (from 0.151 to0.445), and 0.072 (from 0.553 to 0.625), respectively ($n = 52$), and coefficients α_1 and b were significant ($P < 0.05$) in each case. These r^2 values are generally lower than those for solution culture studies, and this reflects the complexity of soils. Indeed, a better prediction was achieved when combined effects of two toxicants (Al^{3+} and H^+) and an ameliorant (Ca^{2+}) were quantified by the equation $RRL = 100 \times RRE_{Al} \times RRE_H \times RRE_{Ca}$ in terms of the dual effects of $\psi_0{}^o$ (data not shown). Regardless, the improvements in the r^2 values demonstrate the importance of the dual effects of $\psi_0{}^o$ upon plant growth. For a reanalysis of published soil studies demonstrating the first effect of $\psi_0{}^o$ in soils, see Kinraide (2006).

Prediction of Ion Uptake and Toxicity with the FIAM, the Surface Ion Activity Model, and Electrostatic Models

All observed values from experiments 1 to 15 were plotted against the values predicted by each model (FIAM, the surface ion activity model [SIAM], the EUM, and the ETM; data not shown). The SIAM considered the effect of $\psi_0{}^o$ on both surface ion activities. The SIAM predictions ($r^2 = 0.861$, $n = 427$ for uptake; $r^2 = 0.802$, $n = 334$ for toxicity) were superior to FIAM predictions ($r^2 = 0.716$ for uptake and $r^2 = 0.721$ for toxicity). The correlations for the electrostatic models ($r^2 = 0.940$ for the EUM and $r^2 = 0.901$ for the ETM), incorporating the effect of $\psi_0{}^o$ on both surface ion activities and $E_{m,surf}$, were superior to the SIAM predictions. These results indicate that the electrostatic models could form the basis for the prediction of

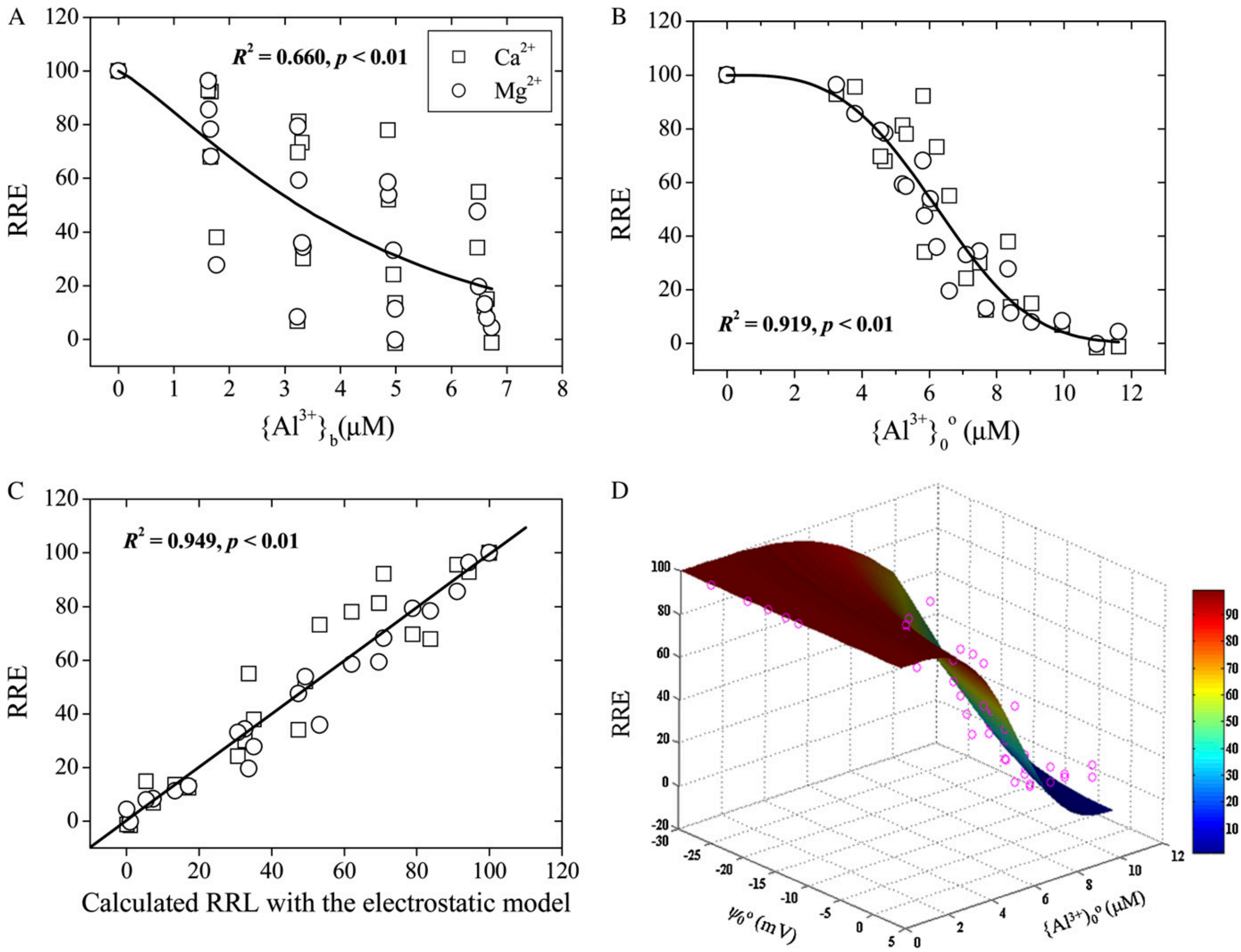

Figure 6. Measured RRE of wheat seedlings exposed to Al^{3+} affected by Ca^{2+} and Mg^{2+}. Data were taken from Kinraide et al. (1992; experiment 14). The RRE is plotted as functions of $\{Al^{3+}\}_b$ (A), $\{Al^{3+}\}_0^o$ (B), or calculated Al^{3+} toxicity based on the ETM (C) or ψ_0^o and $\{Al^{3+}\}_0^o$ (D).

uptake and toxicity of both metal cations and metalloid anions and for the interpretation of other plant-ion interactions. In most cases, the treatment periods in this study ranged from a few minutes (some uptake studies) to a few days (toxicity studies), but studies of longer duration, especially in soils, would certainly be useful for more accurate predictions.

General Evaluation of the Electrostatic Approach to Ion Uptake and Toxicity

The BLM attempts to explain toxicity and alleviation in terms of metal ion binding to cell surface ligands as a key step leading to toxicity. It is proposed in the BLM that alleviation of toxicity by cations is caused by the competition of those ions with the toxic ions for binding to the same ligands. These assumptions may be true but are not verified in most cases. Also, the BLM fails to interpret the enhancement of the uptake and toxicity of arsenate or selenate anions by the treatments that reduce the toxicity of toxic cations (Kinraide, 2003a; Wang et al., 2008). Our study shows that electrostatic mechanisms provide a unified interpretation of both phenomena: the cation reduction of cation uptake and toxicity and the cation enhancement of anion uptake and toxicity.

The alleviation of cation toxicity by site-specific mechanisms, such as competitive binding, may occur in some cases. For example, Weng et al. (2004) and others have noted significant reductions in metal-induced toxicity with reductions in pH in the 6 to 7 range. Such pH reductions would change ψ_0^o by less than 1 mV in most media, a change far too small to account for toxicity reductions. Instead, some key ligands, contributing little to ψ_0^o, such as sites on ion channels or enzymes, may bind H^+ strongly enough for pH shifts from 7 to 6 to be effective. Despite clear evidence for site-specific mechanisms (such as competition), such mechanisms appear to be unimportant in many cases (Kinraide, 2006; Wang et al., 2008). In those cases, including those in this study, the dual effects of ψ_0^{o} are sufficient to explain the ion-toxicant interactions (Kinraide, 2006; Wang et al., 2008; this study).

The GCS model, incorporating the parameter values used by us, appears to be quite robust (Yermiyahu et al., 1997; Zhang et al., 2001; Wang et al., 2008; Kinraide and Wang, 2010), and a fully parameterized GCS model is available from the authors. The model is suitable for the calculation of ψ_0^{o} and for the interpretation of many plant responses to changes in the composition of the aqueous exposure medium.

CONCLUSION

This study provides evidence that PM surface ion activities, as determined by ψ_0^{o}, are often superior to activities in the bulk-phase medium as indicators of plant-ion interactions. This study also indicates that ψ_0^{o} plays an additional role: it is a determinant of $E_{m,surf}$, the electrical component of the driving force for ion uptake. Our findings indicate that these dual effects of ψ_0^{o} play important roles in ion uptake and toxicity in both soil and solution cultures and that the electrostatic uptake and toxicity models provide a novel approach for predicting the uptake and toxicity of both metal cations and metalloid anions. The electrostatic uptake and toxicity models do not negate entirely the BLM. Site-specific competition surely explains some features of ion toxicity and alleviation. Irrespective of whether the mechanisms invoked by the BLM play a role in any given situation, electrostatic effects surely do and should be incorporated into any model, including the BLM, of ion toxicity and the ionic alleviation or enhancement of toxicity.

MATERIALS AND METHODS

Uptake and Toxicity Bioassay Experiments

Data for ion uptake and root elongation in response to the ionic environment were compiled for analysis from previous studies employing solution culture (references in Table I) and soil culture. In addition, data for the uptake and toxicity of copper and As(V) in wheat (*Triticum aestivum*) roots were collected from experiments conducted as part of this study [experiments 3 and 11 for copper and experiments 10 and 15 for As(V)]. The plant species used and a summary of culture conditions are presented in Table I. For detailed experimental methods (except for this study), refer to the corresponding references in Table I.

Experiments 3 and 11: Effects of Ca^{2+}, Mg^{2+}, and pH on Cu^{2+} Uptake and Toxicity

Three sets of uptake and toxicity bioassay experiments were performed, one each for three Ca^{2+} concentrations (0.25, 0.98, and 3.78 mM), three Mg^{2+} concentrations (0.26, 1.0, and 4.0 mM), and three pH values (5.1, 5.5, and 6.0). In each medium, six Cu^{2+} concentrations (0.25–2.0 μM) and a control were tested. Further details of the growth experiments and precautions for the preparation of the test solutions have been presented previously (Wang et al., 2008). For acute toxicity tests, 2-d-old wheat (cv Yangmai 14) seedlings with uniform root length (1–2 cm) were cultured in darkness for 48 h at 25°C in acid-washed polyethylene beakers containing 500 mL of test medium. Each treatment was performed with three or four replicates and eight seedlings per replicate. At termination, the two longest roots of each seedling were measured, and the mean value of 16 measured values per replicate was recorded. The plants were transferred to a 10 mM $Ca(NO_3)_2$ solution for 10 min to remove cell wall-bound copper. Roots were dried at 40°C, weighed, and digested with 5 mL of ultrapure concentrated HNO_3. Copper was determined by flame atomic absorption spectrometry (Varian 220Z).

Experiments 10 and 15: Effects of Ca^{2+}, Mg^{2+}, Na^{+}, and pH on As(V) Uptake and Toxicity

For As(V) uptake, three sets of experiments were performed, one each for three Ca^{2+} concentrations (0.24, 1.0, and 4.1 mM), three Mg^{2+} concentrations (0.26, 0.83, and 3.7 mM), and three pH values (4.4, 5.3, and 6.0). In each medium, five $H_2AsO_4^{-}$ concentrations (0.75–3.0 μM) and a control were tested. For As(V) toxicity experiments, four sets of experiments were performed, one each for Ca^{2+} (0.27–4.3 mM), Mg^{2+} (0.26–4.0 mM), Na^{+} (1.4–20.1 mM), and pH (4.5–6.6). In each medium, five arsenate concentrations (0.67–26.7 μM) and a control were tested. These uptake and growth experiments were similar to experiments 3 and 11. At termination, the plants were transferred to an ice-cold phosphate buffer solution for 10 min to remove cell wall-bound arsenic (Zhang et al., 2009). Roots were dried at 40°C, weighed, and digested with 5 mL of ultrapure concentrated HNO_3. Arsenic was determined by atomic fluorescence spectrometry (AF-160A; Beijing Haichuang Analytical Instrument Co.).

Data Treatment and Statistics

Ion species and activities were calculated using the visual MINTEQ (version 2.51) chemical equilibrium program (U.S. Environmental Protection Agency). The speciation calculations included atmospheric CO_2 ($10^{-3.5}$ atm). Relative root elongation was calculated by the formula RRE = $100(RL_T - RL_S)/(RL_C - RL_S)$, in which RL_T is the mean root length in the presence of toxicants, RL_C is the root length in the corresponding toxicant-free control, and RL_S is root length at the time of seedling transfer to the test medium. Uptake and toxicity were plotted, and curved surfaces were fitted by regression analysis using Origin Professional 6.0 and MATLAB 7.0. Significance levels are $P < 0.05$ for all reported regressions and coefficients.

Received September 13, 2010; accepted November 22, 2010; published November 30, 2010.

LITERATURE CITED

Barber J (1980) Membrane surface charges and potentials in relation to photosynthesis. Biochim Biophys Acta **594:** 253–308

Calabrese EJ (2008) Hormesis: why it is important to toxicology and toxicologists. Environ Toxicol Chem **27:** 1451–1474

Davenport RJ, Reid RJ, Smith FA (1997) Sodium-calcium interactions in two wheat species differing in salinity tolerance. Physiol Plant **99:** 323–327

Di Toro DM, Allen HE, Bergman HL, Meyer JS, Paquin PR, Santore RC (2001) Biotic ligand model of the acute toxicity of metals. 1. Technical basis. Environ Toxicol Chem **20:** 2383–2396

Gage RA, Wijingaarden WV, Theuvenet APR, Borst-Pauwels GWFH, Verkleij AJ (1985) Inhibition of Rb^{+} uptake in yeast by Ca^{2+} is caused by a reduction in the surface potential and not in the Donnan potential of the cell wall. Biochim Biophys Acta **812:** 1–8

Hille B (2001) Ion Channels of Excitable Membranes, Ed 3. Sinauer Associates, Sunderland, MA

Huang JWW, Grunes DL, Kochian LV (1994) Voltage-dependent Ca^{2+} influx into right-side-out plasma membrane vesicles isolated from wheat roots: characterization of a putative Ca^{2+} channel. Proc Natl Acad Sci USA **91:** 3473–3477

Huang JWW, Pellet DM, Papernik LA, Kochian LV (1996) Aluminum interactions with voltage-dependent calcium transport in plasma membrane vesicles isolated from roots of aluminum-sensitive and -resistant wheat cultivars. Plant Physiol **110:** 561–569

Kinraide TB (2001) Ion fluxes considered in terms of membrane-surface electrical potentials. Aust J Plant Physiol **18:** 605–616

Kinraide TB (2003a) The controlling influence of cell-surface electrical potential on the uptake and toxicity of selenate (SeO_4^{2-}). Physiol Plant **117:** 64–71

Kinraide TB (2003b) Toxicity factors in acidic forest soils: attempts to evaluate separately the toxic effects of excessive Al^{3+} and H^+ and insufficient Ca^{2+} and Mg^{2+} upon root elongation. Eur J Soil Sci **54:** 323–333

Kinraide TB (2004) Possible influence of cell walls upon ion concentrations at plasma membrane surfaces: toward a comprehensive view of cell-surface electrical effects upon ion uptake, intoxication, and amelioration. Plant Physiol **136:** 3804–3813

Kinraide TB (2006) Plasma membrane surface potential (psiPM) as a determinant of ion bioavailability: a critical analysis of new and published toxicological studies and a simplified method for the computation of plant psiPM. Environ Toxicol Chem **25:** 3188–3198

Kinraide TB, Parker DR (1987) Cation amelioration of aluminum toxicity in wheat. Plant Physiol **83:** 546–551

Kinraide TB, Ryan PR, Kochian LV (1992) Interactive effects of Al, H, and other cations on root elongation considered in terms of cell-surface electrical potential. Plant Physiol **99:** 1461–1468

Kinraide TB, Wang P (2010) The surface charge density of plant cell membranes (σ): an attempt to resolve conflicting values for intrinsic σ. J Exp Bot **61:** 2507–2518

Kopittke PM, Blamey FPC, Asher CJ, Menzies NW (2010) Trace metal phytotoxicity in solution culture: a review. J Exp Bot **61:** 945–954

Llamas A, Ullrich CL, Sanz A (2000) Cd^{2+} effects on transmembrane electrical potential difference, respiration and membrane permeability of rice (*Oryza sativa* L.) roots. Plant Soil **219:** 21–28

Lock K, Criel P, De Schamphelaere KAC, Van Eeckhout H, Janssen CR (2007a) Influence of calcium, magnesium, sodium, potassium and pH on copper toxicity to barley (*Hordeum vulgare*). Ecotoxicol Environ Saf **68:** 299–304

Lock K, De Schamphelaere KAC, Becaus S, Criel P, Van Eeckhout H, Janssen CR (2007b) Development and validation of a terrestrial biotic ligand model predicting the effect of cobalt on root growth of barley (*Hordeum vulgare*). Environ Pollut **147:** 626–633

Lock K, Van Eeckhout H, De Schamphelaere KAC, Criel P, Janssen CR (2007c) Development of a biotic ligand model (BLM) predicting nickel toxicity to barley (*Hordeum vulgare*). Chemosphere **66:** 1346–1352

Marschner H (1995) Mineral Nutrition of Higher Plants. Academic Press, London

McLaughlin S (1989) The electrostatic properties of membranes. Annu Rev Biophys Biophys Chem **18:** 113–136

Nobel P (1991) Physicochemical and Environmental Plant Physiology. Academic Press, San Diego

Parker DR, Pedler JF, Thomason DN, Li HY (1998) Alleviation of copper rhizotoxicity by calcium and magnesium at defined free metal-ion activities. Soil Sci Soc Am J **62:** 965–972

Peijnenburg WJGM, Posthuma L, Eijsackers HJP, Allen HE (1997) A conceptual framework for implementation of bioavailability of metals for environmental management purposes. Ecotoxicol Environ Saf **37:** 163–172

Pickering IJ, Prince RC, George MJ, Smith RD, George GN, Salt DE (2000) Reduction and coordination of arsenic in Indian mustard. Plant Physiol **122:** 1171–1177

Shomer I, Novacky AJ, Pike SM, Yermiyahu U, Kinraide TB (2003) Electrical potentials of plant cell walls in response to the ionic environment. Plant Physiol **133:** 411–422

Tatulian SA (1999) Surface Electrostatics of Biological Membranes and Ion Binding. Marcel Dekker, New York

Wang P, Zhou DM, Kinraide TB, Luo XS, Li LZ, Li DD, Zhang HL (2008) Cell membrane surface potential (ψ_0) plays a dominant role in the phytotoxicity of copper and arsenate. Plant Physiol **148:** 2134–2143

Weng LP, Wolthoorn A, Lexmond TM, Temminghoff EJM, van Riemsdijk WH (2004) Understanding the effects of soil characteristics on phytotoxicity and bioavailability of nickel using speciation models. Environ Sci Technol **38:** 156–162

Wolt JD (1994) Soil Solution Chemistry: Applications to Environmental Science and Agriculture. Wiley, New York

Wu Y (2007) Bioavailability and rhizotoxicity of trace metals to pea: development of a terrestrial biotic ligand model. PhD thesis. McGill University, Ottawa

Yermiyahu U, Kinraide TB (2005) Binding and electrostatic attraction of trace elements to plant root surfaces. *In* PM Huang, GR Gobran, eds, Biogeochemistry of Trace Elements in the Rhizosphere. Elsevier, Amsterdam, pp 365–389

Yermiyahu U, Rytwo G, Brauer DK, Kinraide TB (1997) Binding and electrostatic attraction of lanthanum (La^{3+}) and aluminum (Al^{3+}) to wheat root plasma membranes. J Membr Biol **159:** 239–252

Zhang Q, Smith FA, Sekimoto H, Reid RJ (2001) Effect of membrane surface charge on nickel uptake by purified mung bean root protoplasts. Planta **213:** 788–793

Zhang X, Zhao FJ, Huang Q, Williams PN, Sun GX, Zhu YG (2009) Arsenic uptake and speciation in the rootless duckweed *Wolffia globosa*. New Phytol **182:** 421–428